ANALYSIS, OPTIMAL CONTROL, AND SIMULATION OF CONDUCTIVE-RADIATIVE HEAT TRANSFER*

Peter Philip[†]

Abstract

This article surveys recent results regarding the existence of weak solutions to quasilinear partial differential equations (PDE) coupled nonlocally by the integral operator of the radiosity equation, modeling conductive-radiative heat transfer. Both the stationary and the transient case are considered. For the stationary case, an optimal control problem with control constraints is presented with first-order necessary optimality conditions, where recent results on the solution theory of the linearized state equation allow to close a previous gap. A finite volume scheme for the discretization of the stationary system is described and, based on this scheme, a numerical computation of the temperature field (solution of the state equation) is shown as well as the numerical solution to a realistic control problem in the context of industrial applications in crystal growth.

MSC: 49K20, 35J60, 35D30, 35K05, 35K55, 45P05, 49J20, 65C20, 80M15, 80M50.

---

keywords: nonlinear elliptic equation, nonlinear parabolic equation, heat equation, nonlocal boundary condition, diffuse-gray radiation, radiosity equation, weak solution, optimal control, finite volume method, numerical simulation

1   Introduction

Modeling and numerical simulation of conductive-radiative heat transfer has become a standard tool to support and improve numerous industrial processes such as crystal growth by the Czochralski method [1] and by the physical vapor transport method [2] to mention just two examples. Moreover, in the context of industrial applications, one is often not only interested in computing stationary or transient temperature fields as they arise from models of conductive-radiative heat transfer, but one also needs to optimize and control such temperature fields according to objective functionals arising from the application [3, 4].

Models including diffuse-gray radiative interactions between cavity surfaces consist of nonlinear elliptic (stationary) or parabolic (transient) PDE (heat equations), where a nonlocal coupling occurs due to the integral operator of the radiosity equation. There have been numerous papers, where the mathematical theory of existence and uniqueness of weak solutions has been developed in recent years (see [5, 6, 7, 8, 9, 10, 11] and references therein). Distributed over several papers, there have been important recent advances reducing regularity requirements on the data [8, 9] as well as improving regularity results for the solution [12].

In the present survey, we compile such results for both the stationary and the transient model. For the stationary model, it is then described, how these results together with advances from [12] regarding the linearized model can be applied to obtain first-order necessary optimality conditions for the optimal control problem considered in [4], closing a gap left open in [4].

We then proceed to the description of a finite volume scheme that has been successfully applied for the numerical solution of conductive-radiative heat transfer models. Numerical solutions based on the finite volume scheme are presented, where the stationary system has been solved for a complex crystal growth arrangement. Finally, numerical results of a related applied optimal control problem are depicted and briefly discussed.

The paper is organized as follows: The model of conductive-radiative

heat transfer is reviewed in Sec. 2.1, surveying some recent improvements regarding the solution of the radiosity equation, which is a key building block of the model. Section 2.2 treats the existence theory of weak solutions, with applications on optimal control in Sec. 3. The finite volume scheme is described in Sec. 4, and we conclude with the numerical results in Sec. 5.

2 Modeling Conductive-Radiative Heat Transfer

2.1 The Model

The space domain $\Omega \subseteq \mathbb{R}^3$ is assumed to consist of two parts Ω_s and Ω_g, where Ω_s represents an opaque solid and Ω_g represents a transparent gas. More precisely, we assume:

(A-1) $\overline{\Omega} = \overline{\Omega}_s \cup \overline{\Omega}_g$, $\Omega_s \cap \Omega_g = \emptyset$, and each of the sets Ω, Ω_s, Ω_g, is a nonvoid, bounded, open subset of $\mathbb{R}^3$ such that the interface surface $\Sigma := \overline{\Omega}_s \cap \overline{\Omega}_g$ is Lipschitz and piecewise C^1, i.e. Σ can be partitioned into finitely many C^1-surfaces.

(A-2) Ω_g is enclosed by Ω_s, i.e. $\Sigma = \partial\Omega_g$ (see Fig. 1).

Heat conduction is considered throughout Ω. Nonlocal radiative heat transport is considered between points on the surface Σ of Ω_g.

Stationary heat conduction is described by

$$- \operatorname{div}\left(\kappa(x,\theta)\,\nabla\,\theta\right) = f(x) \quad \text{in } \Omega, \tag{1}$$

where $\theta(x) \in \mathbb{R}^+$ represents absolute temperature, depending on the space coordinate x; $\kappa > 0$ represents the thermal conductivity, and $f \geq 0$ is a heat source due to some heating mechanism. In practice, for many heating mechanisms such as induction or resistance heating, one has $f = 0$ in Ω_g. One can also allow $f \leq 0$ to model heat sinks due to cooling.

While (1) models the thermal equilibrium, for example, at the end of a heating process, it is often also desirable to model transient heat conduction, for instance, to model crystal growth apparatus during the heating phase, important in situations, where the growth process and possible defect creation is already initiated during the heating phase [13]. Transient heat conduction is described by

$$\frac{\partial\varepsilon(x,\theta)}{\partial t} - \operatorname{div}\left(\kappa(x,\theta)\,\nabla\,\theta\right) = f(t,x) \quad \text{in }]0,T[\times\Omega, \tag{2}$$
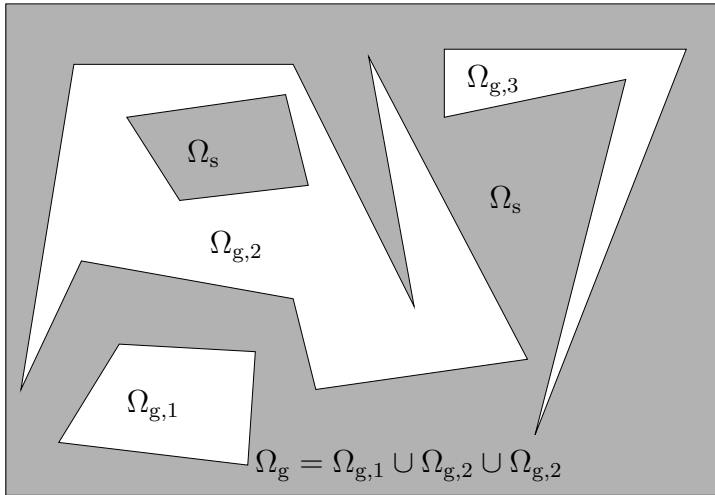
Figure 1: Possible shape of a 2-dimensional section through the 3-dimensional domain $\overline{\Omega} = \overline{\Omega}_s \cup \overline{\Omega}_g$. Here, Ω_g has the 3 connected components $\Omega_{g,1}$, $\Omega_{g,2}$, $\Omega_{g,3}$. Note that, according to (A-2), Ω_g is engulfed by Ω_s, which can not be seen in the 2-dimensional section.

where $T > 0$ represents the final time, θ and f now depend on the time variable t as well as on the space variable x, and $\varepsilon > 0$ represents internal energy.

Remark 1. *If θ is to represent absolute temperature, then it must be always positive. However, it is also mathematically interesting to study equations (1) and (2) in situations, where the solution θ can be negative. For example, negative solutions can occur if the right-hand side function f is allowed to be negative. For that reason, it is often desirable to keep the problem formulation sufficiently flexible, such that it makes sense even if $\theta \geq 0$ can not be guaranteed (considering κ to be defined on $\Omega \times \mathbb{R}$ rather than on $\Omega \times \mathbb{R}^+$ is an example, also cf. Rem. 2 below).*

On the interface Σ between solid and gas, one needs to account for radiosity R and for irradiation J, resulting in a jump in the normal heat flux $\big(\kappa(x,\theta)\,\nabla\,\theta\big) \cdot \vec{n}_g$ according to the following interface condition for (1) (the same works for (2) after replacing the space domains by the corresponding time-space cylinders):

$$\big(\kappa(x,\theta)\,\nabla\,\theta\big)\big\upharpoonright_{\overline{\Omega}_g} \cdot \vec{n}_g + R(\theta) - J(\theta) = \big(\kappa(x,\theta)\,\nabla\,\theta\big)\big\upharpoonright_{\overline{\Omega}_s} \cdot \vec{n}_g \quad \text{on } \Sigma. \qquad (3)$$

Here, $\vec{n}_{\mathrm{g}}$ denotes the unit normal vector pointing from gas to solid and $\upharpoonright$ denotes restriction (or trace). Thus, effectively, (1) consists of two equations, one on Ω_{s} and one on Ω_{g}, coupled via (3) (and analogously for (2)).

It is assumed that the solid is opaque such that $R(\theta)$ and $J(\theta)$ are computed according to the net radiation model for diffuse-gray surfaces, i.e. reflection and emittance are taken to be independent of the angle of incidence and independent of the wavelength. At each point of the surface Σ, the radiosity is the sum of the emitted radiation $E(\theta)$ and of the reflected radiation $J_{\mathrm{r}}(\theta)$:

$$R = E + J_{\mathrm{r}} \ \text{ on } \Sigma. \tag{4}$$

According to the Stefan-Boltzmann law,

$$E(\theta) = \sigma \, \epsilon \, |\theta|^3 \theta \ \text{ on } \Sigma, \tag{5}$$

where $\sigma \in \mathbb{R}^+$ represents the Boltzmann radiation constant, and ϵ represents the potentially material-dependent emissivity of the solid surface. It is assumed that:

(A-3) $\epsilon \in L^\infty(\Sigma)$ with values in $[0,1]$ is such that, for each connected component $\Omega_{\mathrm{g},k}$ of Ω_{g} (cf. Fig. 1), there exists $M_k \subseteq \Sigma_k := \partial \Omega_{\mathrm{g},k}$ such that M_k has positive surface measure and $\epsilon > 0$ on M_k.

Remark 2. *The physically inclined reader might expect to read θ^4 on the right-hand side of (5) rather than $|\theta|^3\theta$. However, whenever $\theta > 0$ does, indeed, represent an absolute temperature, both terms are identical, while, due to its monotonicity properties, $|\theta|^3\theta$ is more suitable for the mathematical theory in situations, where θ can become negative (cf. Rem. 1 above). This remark should be born in mind for each subsequent occurrence of $|\theta|^3\theta$.*

Using the presumed opaqueness together with Kirchhoff's law yields

$$J_{\mathrm{r}} = (1 - \epsilon) \, J. \tag{6}$$

Due to diffuseness, the irradiation can be calculated as

$$J(\theta) = K(R(\theta)), \tag{7}$$

using the nonlocal integral radiation operator K defined by

$$K(\rho)(x) := \int_\Sigma V(x,y)\,\omega(x,y)\,\rho(y)\,\mathrm{d}y \quad \text{for a.e. } x \in \Sigma, \tag{8}$$

$$\omega(x,y) := \frac{\big(\vec{n}_\mathrm{s}(y)\cdot(x-y)\big)\big(\vec{n}_\mathrm{s}(x)\cdot(y-x)\big)}{\pi\big((y-x)\cdot(y-x)\big)^2} \quad \text{for a.e. } (x,y) \in \Sigma\times\Sigma, \tag{9}$$

$$V(x,y) := \begin{cases} 0 & \text{if } \Sigma\cap\,]x,y[\,\neq\emptyset, \\ 1 & \text{if } \Sigma\cap\,]x,y[\,=\emptyset \end{cases} \quad \text{for each } (x,y)\in\Sigma\times\Sigma, \tag{10}$$

where ω is called view factor, V is called visibility factor (being 1 if, and only if, x and y are mutually visible), and $\vec{n}_\mathrm{s}$ denotes the outer unit normal to the solid domain Ω_s, existing almost everywhere on the Lipschitz interface Σ. The following Th. 3 summarizes properties of ω, V, and K, relevant to our considerations.

Theorem 3. *Assume* (A-1) *and* (A-2).

(a) *The kernel $V\omega$ of K is almost everywhere nonnegative (actually positive for $V(x,y)=1$), symmetric, and $V(x,\cdot)\,\omega(x,\cdot)$ is in $L^1(\Sigma)$ with*

$$\int_\Sigma V(x,y)\,\omega(x,y)\,\mathrm{d}y = 1 \quad \text{for a.e. } x\in\Sigma. \tag{11a}$$

Moreover, if Ω_s and Ω_g are polyhedral, then

$$\int_\Sigma V(x,y)\,\omega(x,y)\,\mathrm{d}y > 0 \quad \text{for every } x\in\Sigma, \tag{11b}$$

where one can choose each of the finitely many possible values of $\vec{n}(x)$ if x belongs to more than one face of Σ.

(b) *For each $1\leq p\leq\infty$, the operator $K: L^p(\Sigma) \longrightarrow L^p(\Sigma)$ given by* (8) *is well-defined, linear, bounded, and positive with $\|K\|=1$.*

Proof. See [14, Lem. 1] and [15, Lem. 2]. For (11b), let $\Sigma_z := \{y\in\Sigma : V(z,y)=1\}$, and note that, if Σ is a polyhedral enclosure, then $\mathrm{meas}(\Sigma_z)>0$ for each $z\in\Sigma$. Since $\omega(z,y)>0$ for each $y\in\Sigma_z$, (11b) holds. $\qquad\square$

Remark 4. *It is noted that, for Σ being polyhedral, K is noncompact on $L^p(\Sigma)$ for each $p\in[1,\infty]$, as shown in* [16]. *In settings where the geometry*

of the domains is such that Σ is at least $C^{1,\alpha}$, $\alpha > 0$, K is known to be compact on $L^p(\Sigma)$ [8, 15]. However, it is also shown in [16] that, for $p < \infty$, K can never be compact when reinterpreted as a linear bounded operator $K : L^p(0, T, L^p(\Sigma)) \longrightarrow L^p(0, T, L^p(\Sigma))$ in a transient setting (regardless of the regularity of Σ).

Combining (4) through (7) provides the so-called radiosity equation for R:

$$\big(\operatorname{Id} - (1-\epsilon)K \big)(R) = \epsilon\sigma|\theta|^3\theta, \tag{12}$$

where Id denotes the identity operator. The following Th. 5 allows to solve (12) for R. Its hypothesis involves the technical condition introduced as (A-4).

(A-4) K is compact (Σ being $C^{1,\alpha}$, $\alpha > 0$, is sufficient, cf. Rem. 4) or there exists $r_0 > 0$ such that

$$\operatorname*{ess\,sup}_{x\in\Sigma} \int_{B_{r_0}(x)} V(x,y)\,\omega(x,y)\,\mathrm{d}y \, < 1, \tag{13}$$

where $B_{r_0}(x) := \{y \in \Sigma : \|x - y\|_2 < r_0\}$ (Σ being polyhedral is sufficient for (13) to hold, see [16, Lem. 6]).

Theorem 5. *Let $p \in [1,\infty]$, and assume (A-1) – (A-4). Then the operator $\operatorname{Id} - (1-\epsilon)K$ has an inverse in the Banach space $\mathcal{L}(L^p(\Sigma), L^p(\Sigma))$ of bounded linear operators, and the operator*

$$G := (\operatorname{Id} - K)\big(\operatorname{Id} - (1-\epsilon)K \big)^{-1}\epsilon \tag{14}$$

is an element of $\mathcal{L}(L^p(\Sigma), L^p(\Sigma))$.

Proof. For compact K, see [6, Lem. 2]; for the case that (13) holds, see [16, Th. 5]. □

Corollary 6. *Under the hypotheses of Th. 5, given $\theta \in L^4(\Sigma)$, the radiosity equation (12) has the unique solution $R(\theta) = \big(\operatorname{Id} - (1 - \epsilon)K \big)^{-1}(\epsilon\sigma|\theta|^3\theta) \in L^1(\Sigma)$ (recall $\sigma > 0$ and $\epsilon \in L^\infty(\Sigma)$).* □

Combining (4) – (7) yields

$$R(\theta) - J(\theta) \quad = \quad -\epsilon\big(K(R(\theta)) - \sigma\,|\theta|^3\theta \big) \tag{15a}$$

$$\overset{(12)}{=} \quad (\operatorname{Id} - K)\big(\operatorname{Id} - (1-\epsilon)K \big)^{-1}(\epsilon\sigma|\theta|^3\theta) \tag{15b}$$

$$\overset{(14)}{=} \quad G(\sigma|\theta|^3\theta) \quad \text{on } \Sigma, \tag{15c}$$

such that (3) becomes

$$\left(\kappa(x,\theta)\,\nabla\,\theta\right)\!\restriction_{\overline{\Omega}_{\mathrm{g}}}\cdot\vec{n}_{\mathrm{g}} + G(\sigma|\theta|^{3}\theta) = \left(\kappa(x,\theta)\,\nabla\,\theta\right)\!\restriction_{\overline{\Omega}_{\mathrm{s}}}\cdot\vec{n}_{\mathrm{g}} \quad \text{on }\Sigma. \qquad (16)$$

Assuming the domain Ω is exposed to a black body environment (e.g. a large isothermal room) radiating at θ_{ext} (some given absolute temperature), the Stefan-Boltzmann law provides the outer boundary condition

$$\kappa(x,\theta)\,\nabla\,\theta\cdot\vec{n}_{\mathrm{s}} - \sigma\,\epsilon\,(\theta_{\mathrm{ext}}^{4} - |\theta|^{3}\theta) = 0 \quad \text{on }\partial\Omega. \qquad (17)$$

The outer boundary condition (17) does not allow for nonlocal radiative interactions between open cavities and the outer environment. It is physically reasonable provided the considered domain does not have any open cavities, i.e. under the simplifying assumption:

(A-5) $\overline{\Omega}$ is convex.

One can also omit Assumption (A-5) to include nonlocal radiative interactions between open cavities and the outer environment [17]. Here, (A-5) is used for the sake of simpler notation and briefness.

The summarized stationary model reads

$$- \operatorname{div}\left(\kappa(x,\theta)\,\nabla\,\theta\right) = f(x) \qquad\qquad \text{in }\Omega, \qquad (18a)$$

$$\left(\kappa(x,\theta)\,\nabla\,\theta\right)\!\restriction_{\overline{\Omega}_{\mathrm{g}}}\cdot\vec{n}_{\mathrm{g}} + G(\sigma|\theta|^{3}\theta) = \left(\kappa(x,\theta)\,\nabla\,\theta\right)\!\restriction_{\overline{\Omega}_{\mathrm{s}}}\cdot\vec{n}_{\mathrm{g}} \quad \text{on }\Sigma, \qquad (18b)$$

$$\kappa(x,\theta)\,\nabla\,\theta\cdot\vec{n}_{\mathrm{s}} - \sigma\,\epsilon\,(\theta_{\mathrm{ext}}^{4} - |\theta|^{3}\theta) = 0 \qquad\qquad \text{on }\partial\Omega, \qquad (18c)$$

an integro-differential boundary value problem for the unknown $\theta : \overline{\Omega} \longrightarrow \mathbb{R}$.

The summarized transient model is similar, employing time-dependent variants of the interface and boundary condition, respectively, as well as initial condition (19d):

$$\frac{\partial\varepsilon(x,\theta)}{\partial t} - \operatorname{div}\left(\kappa(x,\theta)\,\nabla\,\theta\right) = f(t,x) \qquad\qquad \text{in }]0,T[\times\Omega, \qquad (19a)$$

$$\left(\kappa(x,\theta)\,\nabla\,\theta\right)\!\restriction_{]0,T[\times\overline{\Omega}_{\mathrm{g}}}\cdot\vec{n}_{\mathrm{g}} + G(\sigma|\theta|^{3}\theta) = \left(\kappa(x,\theta)\,\nabla\,\theta\right)\!\restriction_{]0,T[\times\overline{\Omega}_{\mathrm{s}}}\cdot\vec{n}_{\mathrm{g}}$$
$$\text{on }]0,T[\times\Sigma, \qquad (19b)$$

$$\kappa(x,\theta)\,\nabla\,\theta\cdot\vec{n}_{\mathrm{s}} + \sigma\,\epsilon\,|\theta|^{3}\theta = \sigma\,\epsilon\,\theta_{\mathrm{ext}}^{4} \qquad \text{on }]0,T[\times\partial\Omega, \qquad (19c)$$

$$\theta(0,x) = \theta_{\mathrm{init}}(x) \qquad \text{on }\Omega, \qquad (19d)$$

an integro-differential initial-boundary value problem for the unknown $\theta : [0,T] \times \overline{\Omega} \longrightarrow \mathbb{R}$.

2.2   Existence of Weak Solutions

The assumptions introduced in the previous section were sufficient for the formulation and solution of the radiosity equation (12). For the existence theory of (18) and (19), we need to introduce further conditions on the material and data functions and on the domain.

(A-6) $\kappa : \Omega \times \mathbb{R} \longrightarrow \mathbb{R}^+$ is piecewise continuous in the following sense: There exist finitely many open sets with Lipschitz boundary $\Omega_1, \ldots \Omega_M \subseteq \Omega$ such that

$$\overline{\Omega} = \bigcup_{i=1}^{M} \overline{\Omega}_i, \quad \Omega_i \cap \Omega_j = \emptyset \text{ for } i \neq j, \quad \Omega_i \subseteq \Omega_g \text{ or } \Omega_i \subseteq \Omega_s \text{ for each } i, \tag{20}$$

and there exist continuous functions $\kappa_1, \ldots, \kappa_M : \mathbb{R} \longrightarrow \mathbb{R}^+$ such that $\kappa(x, \theta) = \kappa_i(\theta)$ for each $x \in \Omega_i$.

(A-7) There exist $\kappa_l, \kappa_u \in \mathbb{R}^+$ such that $0 < \kappa_l \leq \kappa \leq \kappa_u$.

(A-8) There exists $\epsilon_l \in {]}0, 1{[}$ such that $0 < \epsilon_l \leq \epsilon \leq 1$.

(A-9) $\theta_{ext} \in L^4(\partial\Omega)$ for (18) and $\theta_{ext} = \theta_{init} = \text{const.}$ for (19).

(A-10) $f \in L^1(\Omega)$ for (18) and $f \in L^1\big({]}0, T{[} \times \Omega\big)$ for (19).

(A-11) $\text{dist}(\Sigma, \partial\Omega) > 0$.

We first consider the stationary case (18), surveying recent results from [12, 18] that extend earlier results from [4, 6] (see [19] for some corrections to [18]). Related results for a wavelength-dependent emissivity can be found in [11].

Notation 7. *For $p, q \in [1, \infty]$, let*

$$V^{p,q}(\Omega) := \big\{ u \in W^{1,p}(\Omega) : u \in L^q(\Sigma \cup \partial\Omega) \big\}. \tag{21}$$

Here, as elsewhere in the paper, we simply write u instead of $\text{tr}(u)$ when considering u on $\Sigma \cup \partial\Omega$, suppressing the trace operator tr.

Definition 8. *Assume* (A-1) – (A-4) *and* (A-6) – (A-11). *Following* [18, *Def. 1.2*], *we define* $\theta \in V^{s,4}(\Omega)$ *for some* $s \in [1, \infty]$ *to be a* weak solution *to* (18) *if, and only if,*

$$\int_\Omega \kappa(\cdot, \theta)\, \nabla\, \theta \cdot \nabla\, \psi + \int_{\partial\Omega} \sigma\epsilon|\theta|^3\theta\psi + \int_\Sigma G(\sigma|\theta|^3\theta)\psi = \int_\Omega f\psi + \int_{\partial\Omega} \sigma\epsilon\theta_{\text{ext}}^4\psi \tag{22}$$

for each $\psi \in V^{s',\infty}(\Omega)$, *where* $s' \in [1, \infty]$ *is the conjugate exponent to* s, *i.e.* $\frac{1}{s} + \frac{1}{s'} = 1$.

Theorem 9. *Assume* (A-1) – (A-4) *and* (A-6) – (A-11).

(a) *If* $f \in L^p(\Omega)$, *where* $p > \frac{9}{7}$ *or just* $p > 1$ *under the additional assumption that* Σ *is* $C^{1,\alpha}$, $\alpha > 0$, *then* (18) *has a weak solution* θ. *If* $f \geq 0$, *then* $\theta \geq \operatorname{ess\,inf} \theta_{\text{ext}}$. *Moreover, regarding the regularity of* θ, *if* $p \geq \frac{3}{2}$ *and* $\theta_{\text{ext}} \in L^8(\partial\Omega)$, *then* $|\theta|^r \in W^{1,2}(\Omega)$ *for each* $r \in [1, \infty[$. *If* $p \in]\frac{9}{7}, \frac{3}{2}[$ *and* $\theta_{\text{ext}} \in L^{8p/(3-p)}(\partial\Omega)$, *then* $\theta \in V^{2,2p/(3-2p)}(\Omega)$ *with* $2p/(3-2p) > 6$. *If* Σ *is* $C^{1,\alpha}$, $\alpha > 0$, $p \in [\frac{6}{5}, \frac{9}{7}]$ *and* $\theta_{\text{ext}} \in L^{8p/(3-p)}(\partial\Omega)$, *then* $\theta \in V^{2,(9-5p)/(3-2p)}(\Omega)$ *with* $5 \leq (9-5p)/(3-2p) \leq 6$. *If* Σ *is* $C^{1,\alpha}$, $\alpha > 0$, $p \in]1, \frac{6}{5}[$ *and* $\theta_{\text{ext}} \in L^{8p/(3-p)}(\partial\Omega)$, *then* $\theta \in V^{3p/(3-p),(9-5p)/(3-2p)}(\Omega)$ *with* $\frac{3}{2} < 3p/(3-p) < 2$.

(b) *If* $f \in L^1(\Omega)$, Σ *is* $C^{1,\alpha}$, $\alpha > 0$, *and* $\epsilon < 1$, *then* (18) *has a weak solution* $\theta \in \bigcap_{s\in[1,\frac{3}{2}[} V^{s,4}(\Omega)$.

(c) *If* $\theta_{\text{ext}} \in L^\infty(\partial\Omega)$, $f \in L^p(\Omega)$ *with* $p > \frac{3}{2}$, *and all* $\partial\Omega_i$ *are* C^1, *then* (18) *has a weak solution* $\theta \in W^{1,q}$ *with* $q := 2p > 3$ *(in particular, the solution is Hölder continuous,* $\theta \in C^\gamma(\overline{\Omega})$, $\gamma > 0$). *This solution is unique provided the functions* $\kappa_1, \ldots, \kappa_M$ *of* (A-6) *are Lipschitz continuous.*

Proof. For (a) see [18, Th. 5.1], for (b) see [18, Th. 6.1], and for (c) see [12, Lem. 3.6] and its proof. □

It remains to discuss the transient case. Here, we survey recent results from [9] that extend earlier results from [6]. For the sake of clarity and briefness, the results in [9] were stated for (19) with a Dirichlet condition instead of (19c). However, the proofs in [9] do carry over to the situation of (19), and Def. 11 and Th. 12 below are formulated in this spirit. A similar transient problem, where the transparent region Ω_{g} was *not* enclosed by the opaque region Ω_{s} was first solved in [5]. Once again, related results for a

wavelength-dependent emissivity can be found in [10]. All the mentioned papers make the additional simplifying assumption that the internal energy function is trivial:

(A-12) $\varepsilon : \Omega \times \mathbb{R} \longrightarrow \mathbb{R}$, $\varepsilon(x, \theta) = \theta$.

Notation 10. *We introduce the abbreviations*

$$Q :=]0, T[\times\Omega, \quad \mathcal{S} :=]0, T[\times\Sigma, \quad \mathcal{C} :=]0, T[\times\partial\Omega, \tag{23}$$

and, for $p, q \in [1, \infty]$, the spaces

$$W_p^{1,0}(Q) := \left\{ u \in L^p(Q) : \partial_{x_i} \in L^p(Q) \text{ for } i = 1, 2, 3 \right\}, \tag{24a}$$

$$W_p^1(Q) := \left\{ u \in W_p^{1,0}(Q) : \partial_t \in L^p(Q) \right\}, \tag{24b}$$

$$\mathcal{V}_0^{p,q}(Q) := \left\{ u \in W_p^{1,0}(Q) : u \in L^q(\mathcal{S} \cup \mathcal{C}) \right\}, \tag{24c}$$

$$\mathcal{V}^{p,q}(Q) := \left\{ u \in W_p^1(Q) : u \in L^q(\mathcal{S} \cup \mathcal{C}) \right\}. \tag{24d}$$

Definition 11. *Assume* (A-1) – (A-4) *and* (A-6) – (A-12). *Following* [9, *Def. 1.1], we define* $\theta \in \mathcal{V}_0^{s,4}(Q)$ *for some* $s \in [1, \infty]$ *to be a* weak solution *to* (19) *if, and only if,*

$$-\int_Q \theta \frac{\partial\psi}{\partial t} + \int_Q \kappa(\cdot, \theta) \nabla\theta \cdot \nabla\psi + \int_\mathcal{C} \sigma\epsilon|\theta|^3\theta\psi + \int_\mathcal{S} G(\sigma|\theta|^3\theta)\psi$$

$$= \int_\Omega \theta_{\text{init}}\psi(0) + \int_Q f\psi + \int_\mathcal{C} \sigma\epsilon\theta_{\text{ext}}^4\psi \tag{25}$$

for each $\psi \in \mathcal{V}^{s',\infty}(Q)$ *with* $\psi(T, \cdot) = 0$ *a.e. in* Ω, *where, as before,* $s' \in [1, \infty]$ *is the conjugate exponent to* s.

The formulations in [9, Ths. 2.1, 2.2] and [9, Lem. 3.1] provide stronger results than the formulation of Th. 12(a) below, which has been simplified for the sake of clarity and briefness.

Theorem 12. *Assume* (A-1) – (A-4) *and* (A-6) – (A-12).

(a) *If* $f \in L^2(Q)$, *then* (19) *has a weak solution* $\theta \in \mathcal{V}_0^{s,5}(Q) \cap C(0, T; L^2(\Omega))$ *and* $\partial_t\theta$ *exists in a distributional sense. This solution is unique provided the functions* $\kappa_1, \ldots, \kappa_M$ *of* (A-6) *are Lipschitz continuous. If* $f \in L^s(Q)$ *for* $s > \frac{5}{2}$, *then* $\theta \in L^\infty(Q)$ *and there is* $c > 0$ *such that*

$$\|\theta\|_{L^\infty(Q)} \leq \max\{|\theta_{\text{ext}}|, |\theta_{\text{init}}|\} + c\|f\|_{L^s(Q)}. \tag{26}$$

(b) *If $f \in L^1(\Omega)$, Σ is $C^{1,\alpha}$, $\alpha > 0$, and $\epsilon < 1$, then (19) has a weak solution $\theta \in \bigcap_{1 \leq p < \frac{5}{4}} \mathcal{V}_0^{p,4}(Q) \cap L^{\infty,1}(Q)$, where*

$$L^{\infty,1}(Q) := \left\{ u \in L^1(Q) : \operatorname*{ess\,sup}_{t \in]0,T[} \int_\Omega |u| < \infty \right\}. \tag{27}$$

Proof. (a) has been shown in Th. 2.1 and Lemmas 3.1, 3.2, 3.3 of [9], also see [9, Rem. 3.4]; (b) has been the subject of [9, Th. 4.1]. $\qquad\square$

3   Optimal Control

When modeling heat transfer for industrial applications such as crystal growth, one is usually not merely interested in determining the temperature distribution θ, but one aims at optimizing θ according to a suitable objective functional. For example, during sublimation growth of silicon carbide, small horizontal temperature gradients in the gas domain Ω_g are desirable to avoid defects of the growing crystal, while sufficiently large vertical temperature gradients are required to guarantee a material transport from the silicon source to the seed crystal [20, 21]. This background led to the optimal control problem considered in [4]:

$$\text{minimize} \quad J(\theta, u) := \frac{1}{2} \int_{\Omega_g} \| \nabla \theta - z \|_2^2 + \frac{\nu}{2} \int_{\Omega_s} u^2 \tag{28a}$$

$$\text{subject to} \quad \text{system (18) with } f = \begin{cases} u & \text{on } \Omega_s, \\ 0 & \text{on } \Omega_g, \end{cases} \tag{28b}$$

$$\text{and} \quad 0 < u_a \leq u \leq u_b \quad \text{in } \Omega_s, \tag{28c}$$

where $z : \Omega_g \longrightarrow \mathbb{R}^3$ is a given desired distribution for the temperature gradient. Here, (28b) imposes the condition of no heat sources in the gas region Ω_g, which is the case for the motivating application of induction heating. The control constraints (28c) reflect the fact that only heating (and no cooling) is considered, and they take into account that, due to technical limitations, an actual heating device can not produce heat sources of arbitrarily large values. Precisely stated, the assumptions on ν, z, u_a, u_b are:

(A-13) $\nu > 0$, $z \in L^2(\Omega_g, \mathbb{R}^3)$.

(A-14) $u_a, u_b \in L^\infty(\Omega_\mathrm{s})$, $0 < u_a \le u_b$.

In view of Th. 9(c), in (28a), we consider the objective functional

$$J : W^{1,2}(\Omega) \times L^2(\Omega_\mathrm{s}) \longrightarrow \mathbb{R}_0^+. \tag{29}$$

Actually, from the point of view of the application, a control problem like (28), where the heat sources f are controlled directly, is only the first step. In practice, the heat sources are generated by a heating mechanism such as induction heating, i.e. f itself is again the solution to some equation. A control problem, where f is obtained as a solution to Maxwell's equations describing induction heating, has been considered in [12]. An even more realistic situation was used for the numerical results of Sec. 5 below.

Definition 13. *Under the assumptions of Th. 9(c), define the* control-to-state operator $S : L^2(\Omega_\mathrm{s}) \longrightarrow W^{1,q}(\Omega) \subseteq C^\gamma(\overline{\Omega}) \subseteq L^\infty(\Omega)$ *(*$q > 3$ *as in Th. 9(c), $\gamma > 0$), $u \mapsto \theta$, assigning to $u \in L^2(\Omega_\mathrm{s})$ the unique weak solution θ of (18) with* $f := \begin{cases} u & on\ \Omega_\mathrm{s}, \\ 0 & on\ \Omega_\mathrm{g}, \end{cases}$ *provided by Th. 9(c).*

Definition 14. *Employing the control-to-state operator of Def. 13, and letting*

$$U_\mathrm{ad} := \big\{ u \in L^\infty(\Omega_\mathrm{s}) : u_a \le u \le u_b \big\}, \tag{30}$$

$(\bar\theta, \bar u) \in W^{1,q}(\Omega) \times U_\mathrm{ad}$ *(*$q > 3$ *as in Th. 9(c)) is called an* optimal control *for (28) if, and only if, $\bar\theta = S(\bar u)$, and $\bar u$ minimizes the reduced objective functional*

$$j : L^2(\Omega_\mathrm{s}) \longrightarrow \mathbb{R}_0^+, \quad j(u) := J\big(S(u), u\big) \tag{31}$$

on U_ad.

The following theorem provides the existence of an optimal control for (28) under the simplifying assumption of θ-independent κ:

Theorem 15. *Under the assumptions of Th. 9(c) plus (A-13), (A-14), $\kappa_i = const.$, and $\operatorname{ess\,inf} \theta_\mathrm{ext} > 0$, there exists an optimal control $(\bar\theta, \bar u)$ for (28).*

Proof. See [4, Th. 5.2]. $\qquad\square$

Theorem 18 below provides the differentiability of the control-to-state operator as well as first-order necessary optimality conditions for (28), which

are related to weak solutions to the linearized form of (18) as defined in
Def. 16 below. For the situation of Th. 15, variants of Ths. 17 and 18
below had already been considered in [4], where the Fredholm alternative
was employed to show the linearized form of (18) admits a unique solution,
provided the homogeneous version admits only 0 as its solution. However,
the latter question remained open in [4]. This gap has now been closed due
to the availability of [12, Th. 4.4].

While the existence of an optimal control for (28) has only been proved
for θ-independent κ, the following theory of first-order necessary optimality
conditions merely requires the much milder condition:

(A-15) Each of the functions $\kappa_1, \ldots, \kappa_M$ of (A-6) are Lipschitz continuous and
continuously differentiable (i.e. C^1 with bounded derivative).

Definition 16. *Under the assumptions of Th. 9(c) plus* $\operatorname{ess\,inf} \theta_{\mathrm{ext}} > 0$ *and*
(A-15), *let* $\bar{u} \in L^2(\Omega_{\mathrm{s}})$, $\bar{u} \geq 0$, $\bar{\theta} := S(\bar{u}) \in W^{1,q}(\Omega)$ *with* $q > 3$ *as in Th.*
9(c). Given $\mathcal{F}$ *in the dual of* $W^{1,q'}(\Omega)$ *(q' the conjugate exponent to q), a*
function $\theta \in W^{1,q}(\Omega)$ *is called a* weak solution *to the* linearized form of (18)
(or (22)) with right-hand side $\mathcal{F}$ *if, and only if,*

$$
\int_\Omega \kappa(\cdot, \bar{\theta})\, \nabla\theta \cdot \nabla\psi + \int_\Omega \frac{\partial\kappa}{\partial\theta}(\cdot, \bar{\theta})\theta\,\nabla\bar{\theta}\cdot\nabla\psi
$$
$$
+ 4\int_{\partial\Omega} \sigma\epsilon|\bar{\theta}|^3\theta\psi + 4\int_\Sigma G(\sigma|\bar{\theta}|^3\theta)\psi = \mathcal{F}(\psi) \tag{32}
$$

for each $\psi \in W^{1,q'}(\Omega)$ *(recall* $G : L^\infty(\Sigma) \longrightarrow L^\infty(\Sigma)$ *according to Th. 5).*

Theorem 17. *In the situation of Def. 16, there exists a unique weak solution*
to the linearized form of (18), i.e. $\theta \in W^{1,q}(\Omega)$ *such that (32) holds for each*
$\psi \in W^{1,q'}(\Omega)$. *Moreover, there exists* $c > 0$ *such that*

$$
\|\theta\|_{W^{1,q}(\Omega)} \leq c\,\|\mathcal{F}\|. \tag{33}
$$

Proof. See [12, Th. 4.4]. The proof is based on the Fredholm alternative,
which yields that (32) admits a unique solution $\theta \in W^{1,q}(\Omega)$ if, and only if,
its homogeneous version ($\mathcal{F} = 0$) has 0 as its unique solution. The latter is
established in the proof of [12, Th. 4.4] via a comparison principle. $\square$

Theorem 18. *Under the assumptions of Th. 9(c) plus* $\operatorname{ess\,inf} \theta_{\mathrm{ext}} > 0$ *and*
(A-15), *the control-to-state operator of Def. 13 is Fréchet differentiable on*

$L_+^2(\Omega_s) := \{\bar{u} \in L^2(\Omega_s) : \bar{u} > 0\}$. *Moreover, for* $\bar{u} \in L_+^2(\Omega_s)$, $\bar{\theta} = S(\bar{u})$, *and* $u \in L^2(\Omega_s)$, *one has* $\theta := S'(\bar{u})(u)$ *given by the weak solution to the linearized form of* (18) *with right-hand side* $\mathcal{F}(\psi) := \mathcal{F}_u(\psi) := \int_{L^2(\Omega_s)} u\psi$.

If (A-13) *and* (A-14) *hold, then* $(\bar{\theta}, \bar{u}) \in W^{1,q}(\Omega) \times U_{ad}$ *(*$q > 3$ *as in Th. 9(c)) being an optimal control for* (28) *implies the necessary condition*

$$j'(\bar{u})(u-\bar{u}) = \langle \nabla \bar{\theta} - z, \nabla \theta \rangle_{L^2(\Omega_g)} + \nu \langle \bar{u}, (u-\bar{u}) \rangle_{L^2(\Omega_s)} \geq 0 \quad \text{for each } u \in U_{ad}, \tag{34}$$

with j *as in* (31), $\bar{\theta} = S(\bar{u})$, *and* $\theta = S'(\bar{u})(u - \bar{u})$.

Proof. Using Th. 17, the proof is based on the implicit function theorem and can be conducted as in [4, Th. 7.1]. □

Second-order sufficient optimality conditions for the situation of Th. 15 have been proved in [22], and a similar problem with constraints on θ (i.e. state constraints) has been treated in [23].

4 Finite Volume Discretization

4.1 Setting

The numerical simulation results presented in Sec. 5 below are based on a finite volume discretization of (18), which is described in the present section. As for the considerations on optimal control, we will restrict ourselves to the stationary setting. For transient simulation results solving (19), we refer to [24, 25, 26]. Descriptions of finite volume schemes suitable for the transient situation can be found in [17, 24].

The described finite volume scheme was designed for polyhedral domains. In consequence, within the present section, assume:

(A-16) Ω_g and Ω_s are polyhedral.

For the sake of more readable notation, we use the following simplified version of (A-6):

(A-17) There are precisely two materials, i.e. (A-6) holds with $M = 2$, $\Omega_1 = \Omega_g$, $\Omega_2 = \Omega_s$.

We also impose more regularity on the emissivity, the external temperature, and the heat sources:

(A-18) $\epsilon : \Sigma \longrightarrow [0,1]$ and $\theta_{\mathrm{ext}} : \partial\Omega \longrightarrow \mathbb{R}^+$ are continuous. Moreover, there are continuous functions $f_m : \overline{\Omega}_m \longrightarrow \mathbb{R}$ such that $f_m \!\upharpoonright_{\Omega_m} = f \!\upharpoonright_{\Omega_m}$, $m \in \{\mathrm{s},\mathrm{g}\}$.

4.2   Discretization of the Local Terms

An admissible discretization of Ω is given by a finite family $\mathcal{T} := (\omega_i)_{i \in I}$ of subsets of Ω satisfying a number of assumptions, subsequently denoted by (DA-$*$).

(DA-1) $\mathcal{T} = (\omega_i)_{i \in I}$ forms a finite partition of Ω (i.e. $\overline{\Omega} = \bigcup_{i \in I} \overline{\omega}_i$), and, for each $i \in I$, ω_i is a nonvoid, polyhedral, connected, and open subset of Ω.

From $\mathcal{T}$, one can define discretizations of Ω_{s} and Ω_{g}: For $m \in \{\mathrm{s},\mathrm{g}\}$ and $i \in I$, let

$$\omega_{m,i} := \omega_i \cap \Omega_m, \quad I_m := \big\{ j \in I : \omega_{m,j} \neq \emptyset \big\}, \quad \mathcal{T}_m := (\omega_{m,i})_{i \in I_m}. \quad (35)$$

To allow the incorporation of the interface condition (18b) into the scheme, it is assumed that, if some $\overline{\omega}_i$ has a 2-dimensional intersection with the interface Σ, then it lies on both sides of the intersection. More precisely:

(DA-2) For each $i \in I$: $\partial_{\mathrm{reg}}\omega_{\mathrm{s},i} \cap \Sigma = \partial_{\mathrm{reg}}\omega_{\mathrm{g},i} \cap \Sigma$, where ∂_{reg} denotes the regular boundary of a polyhedral set, i.e. the parts of the boundary, where a unique outer unit normal vector exists (see Fig. 2), $\partial_{\mathrm{reg}}\emptyset :=$ $\emptyset$.

Integrating (18a) over $\omega_{m,i}$ and applying the Gauss-Green integration theorem yields

$$-\int_{\partial\omega_{m,i}} \kappa_m(\theta)\, \nabla\,\theta \cdot \vec{n}_{\omega_{m,i}} = \int_{\omega_{m,i}} f, \qquad (36)$$

where $\vec{n}_{\omega_{m,i}}$ denotes the outer unit normal vector to $\omega_{m,i}$.

The finite volume scheme is furnished by incorporating the interface and boundary conditions (18b) and (18c) followed by an approximation of the integrals by quadrature formulas. To approximate θ by a finite number of discrete unknowns θ_i, $i \in I$, precisely one value θ_i is associated with each control volume ω_i. Introducing a discretization point $x_i \in \omega_i$ for each control volume ω_i, the θ_i can be interpreted as $\theta(x_i)$. Moreover, the discretization
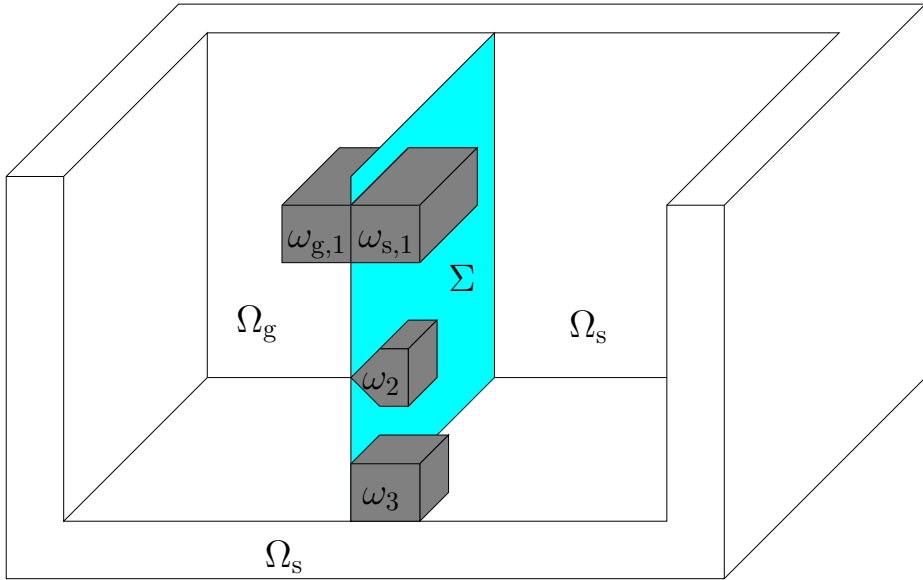
Figure 2: Illustration of condition (DA-2): Ω_s consists of the outer wall of the box as well as of the region to the right of the vertical plane in the middle of the box, which is contained in Σ; Ω_g consists of the region to the left of that plane and engulfed by the wall. Both ω_1 and ω_2 satisfy (DA-2) (since $\partial_{reg}\omega_{s,2} \cap \Sigma = \emptyset$ and $\partial_{reg}\omega_{g,2} \cap \Sigma = \partial_{reg}\emptyset \cap \Sigma = \emptyset$), however ω_3 does not satisfy (DA-2) (since $\partial_{reg}\omega_{s,3} \cap \Sigma \neq \emptyset$ and $\partial_{reg}\omega_{g,3} \cap \Sigma = \partial_{reg}\emptyset \cap \Sigma = \emptyset$).

makes use of regularity assumptions concerning the partition $(\omega_i)_{i \in I}$ that can be expressed in terms of the x_i (see (DA-3), (DA-4), and (DA-5) below).

The boundary of each control volume $\omega_{m,i}$ can be decomposed according to (see Fig. 3)

$$\partial\omega_{m,i} = \left(\partial\omega_{m,i} \cap \Omega_m\right) \cup \left(\partial\omega_{m,i} \cap \partial\Omega\right) \cup \left(\partial\omega_{m,i} \cap \Sigma\right). \qquad (37)$$

To guarantee that there is a discretization point x_i in each of the integration domains occurring in (37), it is assumed that the discretization $\mathcal{T}$ respects interfaces and outer boundaries in the following sense:

(DA-3) For each $m \in \{s, g\}$, $i \in I_m$: $x_i \in \overline{\omega}_{m,i}$. In particular, if $\omega_{s,i} \neq \emptyset$ and $\omega_{g,i} \neq \emptyset$, then $x_i \in \overline{\omega}_{s,i} \cap \overline{\omega}_{g,i}$.

(DA-4) For each $i \in I$, the following holds: If $\operatorname{meas}(\overline{\omega}_i \cap \partial\Omega) \neq 0$, then $x_i \in \overline{\omega}_i \cap \partial\Omega$ (cf. Fig. 4).
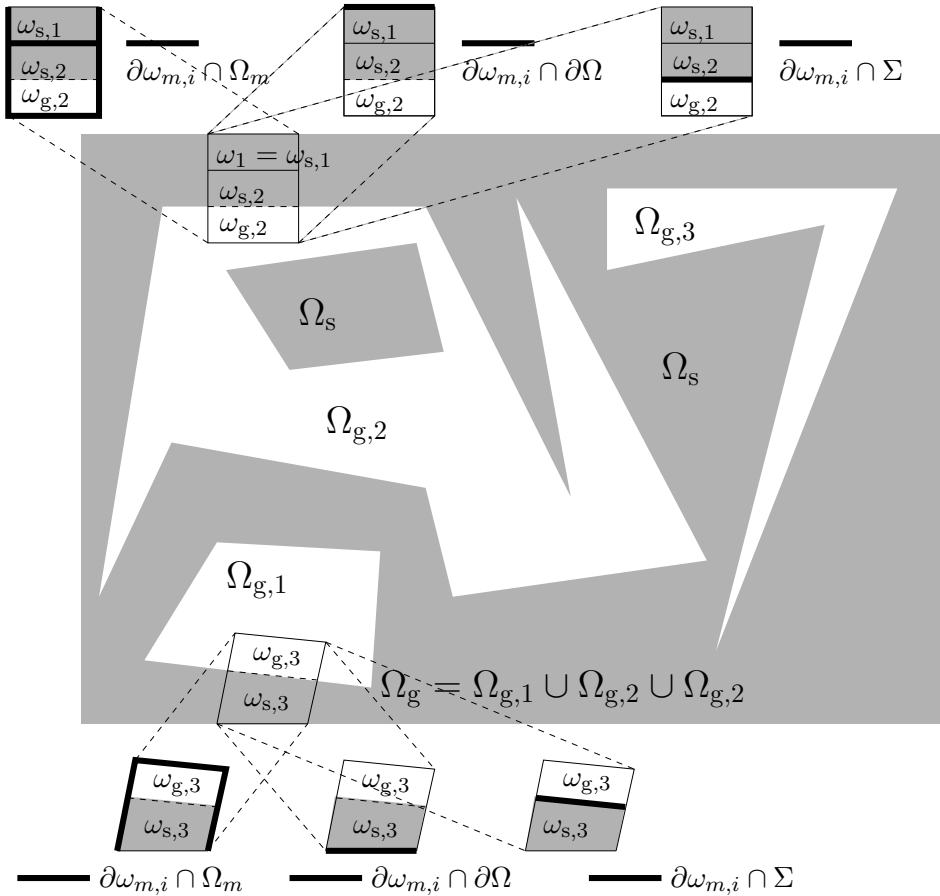
Figure 3: Illustration of the decomposition of the boundary of control volumes $\omega_{m,i}$ according to (37). The lower control volume ω_3 is not admissible, as it has 2-dimensional intersections with both Σ and $\partial\Omega$ (see Rem. 19).

Remark 19. *Suppose a control volume $\overline{\omega}_i$ has a 2-dimensional intersection with both $\partial\Omega$ and Σ. Then, by (DA-2), $\omega_{s,i} \neq \emptyset$ and $\omega_{g,i} \neq \emptyset$. Thus, by (DA-3), $x_i \in \Sigma$. On the other hand, by (DA-4), $x_i \in \partial\Omega$, which means that (A-11) is violated. It is thus shown that $\overline{\omega}_i$ cannot have 2-dimensional intersections with both $\partial\Omega$ and Σ. In particular, the lower control volume ω_3 in Fig. 3 is not admissible.*
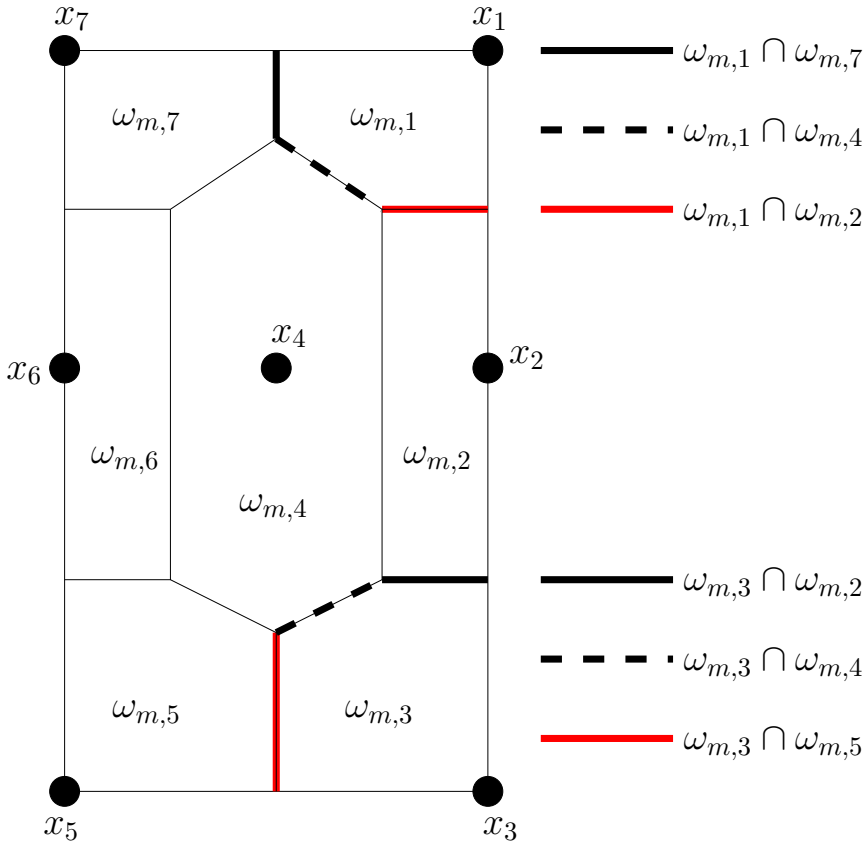
Figure 4: Illustration of conditions (DA-4) and (DA-5) as well as of the partition of $\partial\omega_{m,i} \cap \Omega_m$ according to (40). One has $\mathrm{nb}_m(1) = \{2, 4, 7\}$ and $\mathrm{nb}_m(3) = \{2, 4, 5\}$.

Using the boundary condition (18c) leads to the following approximation:

$$-\int_{\partial\omega_{s,i}\cap\partial\Omega} \kappa_s(\theta)\,\nabla\theta\cdot\vec{n}_{\omega_{s,i}} \approx -\sigma\,\epsilon(x_i)\,(\theta_{\mathrm{ext}}^4(x_i) - |\theta_i|^3\theta_i)\,\mathrm{meas}\left(\partial\omega_{s,i}\cap\partial\Omega\right).$$

$$(38)$$

The nonlocal interface condition (18b) with $G(\sigma|\theta|^3\theta) = -\epsilon\left(K(R(\theta)) - \sigma|\theta|^3\theta\right)$ according to (15) yields

$$-\sum_{m\in\{s,g\}}\int_{\partial\omega_{m,i}\cap\Sigma} \kappa_m(\theta)\,\nabla\theta\cdot\vec{n}_{\omega_{m,i}} = -\int_{\omega_i\cap\Sigma}\epsilon\left(K(R(\theta)) - \sigma|\theta|^3\theta\right).\quad(39)$$

The approximation of the nonlocal term $K(R(\theta))$ is more involved and will be considered in detail in Sec. 4.3 below. First, to approximate the integrals over $\partial\omega_{m,i} \cap \Omega_m$, this set is partitioned further (see Fig. 4):

$$\partial\omega_{m,i} \cap \Omega_m = \bigcup_{j\in\mathrm{nb}_m(i)} \partial\omega_{m,i} \cap \partial\omega_{m,j}, \tag{40}$$

where $\mathrm{nb}_m(i) := \{j \in I_m \setminus \{i\} : \mathrm{meas}(\partial\omega_{m,i} \cap \partial\omega_{m,j}) \neq 0\}$ is the set of m-neighbors of i. Moreover, it is assumed that:

(DA-5) For each $i \in I$, $j \in \mathrm{nb}(i) := \{j \in I \setminus \{i\} : \mathrm{meas}(\partial\omega_i \cap \partial\omega_j) \neq 0\}$: $x_i \neq x_j$ and $\frac{x_j - x_i}{\|x_i - x_j\|_2} = \vec{n}_{\omega_i} \restriction_{\partial\omega_i \cap \partial\omega_j}$, where $\vec{n}_{\omega_i} \restriction_{\partial\omega_i \cap \partial\omega_j}$ is the restriction of the normal vector $\vec{n}_{\omega_i}$ to the interface $\partial\omega_i \cap \partial\omega_j$. Thus, the line segment joining neighboring vertices x_i and x_j is always perpendicular to $\partial\omega_i \cap \partial\omega_j$ (see Fig. 4, where the vertices x_i are chosen such that (DA-5) is satisfied).

The approximation of the integrals over $\partial\omega_{m,i} \cap \Omega_m$, is now provided by replacing the normal gradient of θ on $\partial\omega_i \cap \partial\omega_j$ by the corresponding difference quotient and by approximating $\kappa_m(\theta)$ on $\partial\omega_{m,i} \cap \partial\omega_{m,j}$ by the arithmetic mean of $\kappa_m(\theta_i)$ and $\kappa_m(\theta_j)$:

$$\int_{\partial\omega_{m,i}\cap\Omega_m} \kappa_m(\theta)\,\nabla\theta\cdot\vec{n}_{\omega_{m,i}}$$
$$\approx \sum_{j\in\mathrm{nb}_m(i)} \frac{\kappa_m(\theta_i) + \kappa_m(\theta_j)}{2}\,\frac{\theta_j - \theta_i}{\|x_i - x_j\|_2}\,\mathrm{meas}\left(\partial\omega_{m,i}\cap\partial\omega_{m,j}\right). \tag{41}$$

Finally, for the approximation of the source term,

$$\int_{\omega_{m,i}} f \approx f_m(x_i)\,\mathrm{meas}(\omega_{m,i}). \tag{42}$$

4.3   Discretization of the Nonlocal Radiation Terms

Similarly to the finite volume approximation of the local terms, the discretization of $K(R(\theta))$ proceeds by partitioning the surface Σ into 2-dimensional polyhedral control volumes (so-called boundary elements).

(DA-6) $(\zeta_\alpha)_{\alpha\in I_\Sigma}$ is a finite partition of Σ, where for each $\alpha \in I_\Sigma$, the boundary element ζ_α is a nonvoid, polyhedral, connected, and (relative) open subset of Σ, lying in a 2-dimensional affine subspace of $\mathbb{R}^3$.

On Σ, the boundary elements are supposed to be compatible with the control volumes ω_i:
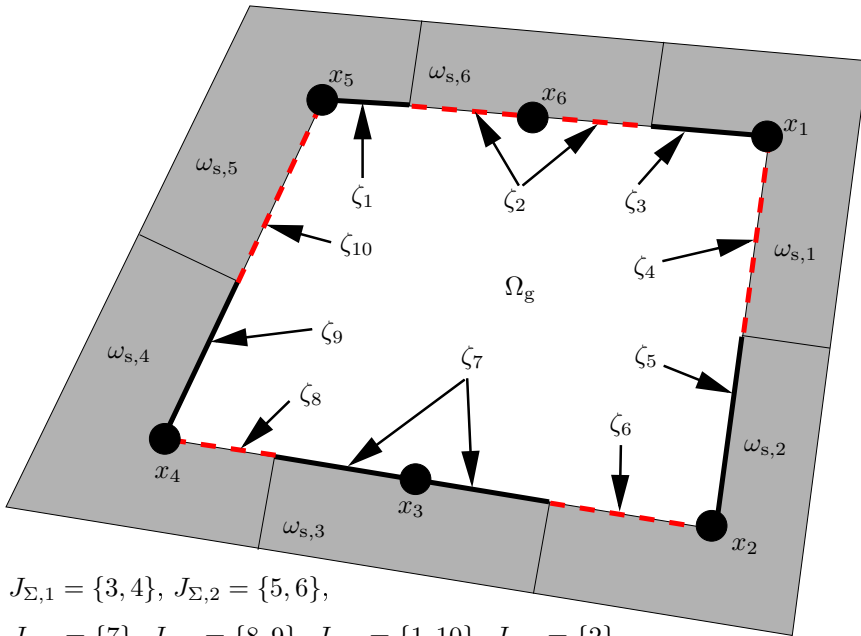
(DA-7) For each $\alpha \in I_\Sigma$, there is a unique $i(\alpha) \in I$ such that $\zeta_\alpha \subseteq \partial\omega_{\mathrm{s},i(\alpha)} \cap \Sigma$. Moreover, for each $\alpha \in I_\Sigma$: $x_{i(\alpha)} \in \overline{\zeta}_\alpha$ (see Fig. 5).

Definition and Remark 20. *For each $i \in I$, define $J_{\Sigma,i} := \{\alpha \in I_\Sigma : \mathrm{meas}(\zeta_\alpha \cap \partial\omega_{\mathrm{s},i}) \neq 0\}$. It then follows from (DA-1), (DA-6), and (DA-7), that $(\zeta_\alpha \cap \partial\omega_{\mathrm{s},i})_{\alpha \in J_{\Sigma,i}}$ is a partition of $\partial\omega_{\mathrm{s},i} \cap \Sigma = \overline{\omega}_i \cap \Sigma$ (see Fig. 5).*

$$i(1) = i(10) = 5,\ i(2) = 6,\ i(3) = i(4) = 1,$$
$$i(5) = i(6) = 2,\ i(7) = 3,\ i(8) = i(9) = 4.$$

$J_{\Sigma,1} = \{3,4\},\ J_{\Sigma,2} = \{5,6\},$

$J_{\Sigma,3} = \{7\},\ J_{\Sigma,4} = \{8,9\},\ J_{\Sigma,5} = \{1,10\},\ J_{\Sigma,6} = \{2\}.$

Figure 5: Illustration of the partitioning of Σ into the ζ_α, and of the compatibility condition (DA-7) as well as of Def. and Rem. 20. Note that, in order to satisfy (DA-2), each ω_i must extend into Ω_{g} (i.e. $\omega_{\mathrm{g},i} \neq \emptyset$). However, only the parts $\omega_{\mathrm{s},i}$ are drawn in the figure.

The radiosity $R(\theta)$ is approximated as constant on each boundary element ζ_α, $\alpha \in I_\Sigma$. The approximated value is denoted by $R_\alpha(\vec{u})$, depending on the

vector $\vec{u} := (\theta_{i(\alpha)})_{\alpha \in I_\Sigma}$. From (8), one obtains

$$\int_{\zeta_\alpha} K(R(\theta)) \approx \sum_{\beta \in I_\Sigma} R_\beta(\vec{u}) \, V_{\alpha,\beta} \quad \text{for each } \alpha \in I_\Sigma, \tag{43}$$

where

$$V_{\alpha,\beta} := \int_{\zeta_\alpha \times \zeta_\beta} V \, \omega \quad \text{for each } (\alpha, \beta) \in I_\Sigma \times I_\Sigma. \tag{44}$$

The $V_{\alpha,\beta}$ are nonnegative since $V\omega$ is nonnegative according to Th. 3(a). The forms of V and ω imply the symmetry condition

$$V_{\alpha,\beta} = V_{\beta,\alpha} \quad \text{for each } (\alpha, \beta) \in I_\Sigma \times I_\Sigma, \tag{45}$$

and (11a) implies

$$\sum_{\beta \in I_\Sigma} V_{\alpha,\beta} = \text{meas}(\zeta_\alpha) \quad \text{for each } \alpha \in I_\Sigma. \tag{46}$$

Using (43) and approximating ϵ as constant on ζ_α allows to write the radiosity equation in the integrated and discretized form

$$R_\alpha(\vec{u}) \, \text{meas}(\zeta_\alpha) - \big(1 - \epsilon(x_{i(\alpha)})\big) \sum_{\beta \in I_\Sigma} R_\beta(\vec{u}) \, V_{\alpha,\beta}$$

$$= \sigma \, \epsilon(x_{i(\alpha)}) \, |\theta_{i(\alpha)}|^3 \theta_{i(\alpha)} \, \text{meas}(\zeta_\alpha) \quad \text{for each } \alpha \in I_\Sigma. \tag{47}$$

If the vector $\vec{u} = (\theta_{i(\alpha)})_{\alpha \in I_\Sigma}$ is known, then (47) constitutes a linear system for the determination of the vector $(R_\alpha(\vec{u}))_{\alpha \in I_\Sigma}$.

In matrix form, (47) reads

$$\mathbf{G}\,\vec{R}(\vec{u}) = \vec{E}(\vec{u}), \tag{48}$$

with vector-valued functions

$$\vec{R}: \mathbb{R}^{I_\Sigma} \longrightarrow \mathbb{R}^{I_\Sigma}, \qquad \vec{R}(\vec{u}) = \big(R_\alpha(\vec{u})\big)_{\alpha \in I_\Sigma}, \tag{49a}$$

$$\vec{E}: \mathbb{R}^{I_\Sigma} \longrightarrow \mathbb{R}^{I_\Sigma}, \qquad \vec{E}(\vec{u}) = \big(E_\alpha(\vec{u})\big)_{\alpha \in I_\Sigma},$$

$$E_\alpha(\vec{u}) := \sigma \, \epsilon(x_{i(\alpha)}) \, |u_\alpha|^3 u_\alpha \, \text{meas}(\zeta_\alpha), \tag{49b}$$

and the matrix

$$\mathbf{G} = (G_{\alpha,\beta})_{(\alpha,\beta) \in I_\Sigma^2}, \quad G_{\alpha,\beta} := \begin{cases} \text{meas}(\zeta_\alpha) - \big(1 - \epsilon(x_{i(\alpha)})\big) V_{\alpha,\beta} & \text{for } \alpha = \beta, \\ - \big(1 - \epsilon(x_{i(\alpha)})\big) V_{\alpha,\beta} & \text{for } \alpha \neq \beta. \end{cases} \tag{49c}$$

Lemma 21. (a) *For each $\alpha \in I_\Sigma$: $\sum_{\beta \in I_\Sigma \setminus \{\alpha\}} |G_{\alpha,\beta}| \leq (1 - \epsilon(x_{i(\alpha)})) G_{\alpha,\alpha} \leq G_{\alpha,\alpha}$. In particular, $\mathbf{G}$ is weakly diagonally dominant.*

(b) $\mathbf{G}$ *is an M-matrix, i.e.* $\mathbf{G}$ *is invertible,* $\mathbf{G}^{-1}$ *is nonnegative, and* $G_{\alpha,\beta} \leq 0$ *for each* $(\alpha, \beta) \in I_\Sigma^2$, $\alpha \neq \beta$.

Proof. See [17, Lem. 3.4 and Rem. 3.5]. $\qquad\square$

Now, Lemma 21(b) allows to give a precise definition of $\vec{R}$ by completing (49a) with

$$\vec{R}(\vec{u}) := \mathbf{G}^{-1}\left(\vec{E}(\vec{u})\right). \tag{50}$$

Remark 22. *The definition of $\vec{R}$ in (50) implies that (47) and (48) hold with $\vec{u} = (\theta_{i(\alpha)})_{\alpha \in I_\Sigma}$ replaced by a general vector $\vec{u} = (u_\alpha)_{\alpha \in I_\Sigma} \in \mathbb{R}^{I_\Sigma}$.*

Finally, introducing the vector-valued function

$$\begin{aligned}
\vec{V} : \mathbb{R}^{I_\Sigma} &\longrightarrow \mathbb{R}^{I_\Sigma}, \qquad \vec{V}(\vec{u}) = \left(V_\alpha(\vec{u})\right)_{\alpha \in I_\Sigma}, \\
V_\alpha(\vec{u}) &:= \epsilon(x_{i(\alpha)}) \sum_{\beta \in I_\Sigma} R_\beta(\vec{u}) \, V_{\alpha,\beta},
\end{aligned} \tag{51}$$

(43) provides the desired approximation of the nonlocal term in (39):

$$\int_{\zeta_\alpha} \epsilon \, K(R(\theta)) \approx \epsilon(x_{i(\alpha)}) \sum_{\beta \in I_\Sigma} R_\beta(\vec{u}) \, V_{\alpha,\beta} = V_\alpha(\vec{u}). \tag{52}$$

The following Lem. 23 states some useful properties of the function $\vec{V}$. We introduce the following notation for $\vec{u} = (u_i)_{i \in I_\Sigma} \in \mathbb{R}^{I_\Sigma}$:

$$\min(\vec{u}) := \min\{u_i : i \in I_\Sigma\}, \quad \max(\vec{u}) := \max\{u_i : i \in I_\Sigma\}. \tag{53}$$

Lemma 23. (a) *For each $\vec{u} \in (\mathbb{R}_0^+)^{I_\Sigma}$: $\vec{R}(\vec{u}) \geq 0$ and $\vec{V}(\vec{u}) \geq 0$.*

(b) *For each $\vec{u} \in (\mathbb{R}_0^+)^{I_\Sigma}$, $\alpha \in I_\Sigma$:*

$$\sigma \, \epsilon(x_{i(\alpha)}) \, \min(\vec{u})^4 \, \mathrm{meas}(\zeta_\alpha) \leq V_\alpha(\vec{u}) \leq \sigma \, \epsilon(x_{i(\alpha)}) \, \max(\vec{u})^4 \, \mathrm{meas}(\zeta_\alpha).$$

Proof. See [17, Lem. 3.7]. $\qquad\square$

4.4   The Finite Volume Scheme

For $\vec{u} = (u_i)_{i \in I}$, define
$$\vec{u} \restriction_{I_\Sigma} := (u_{i(\alpha)})_{\alpha \in I_\Sigma}. \tag{54}$$

At this point, all preparations are in place to state the finite volume scheme in (55) below. The terms in (55) arise from (36) after summing over $m \in \{s, g\}$ and employing the approximations (38), (39), (41), (42), and (52), respectively. One is seeking a solution $\vec{u} = (u_i)_{i \in I}$, to

$$0 = - \sum_{m \in \{s,g\}} \sum_{j \in \mathrm{nb}_m(i)} \frac{\kappa_m(u_i) + \kappa_m(u_j)}{2} \frac{u_j - u_i}{\|x_i - x_j\|_2} \, \mathrm{meas}\left(\partial\omega_{m,i} \cap \partial\omega_{m,j}\right) \tag{55a}$$

$$+ \, \sigma \, \epsilon(x_i) \left(u_i^4 - \theta_{\mathrm{ext}}^4(x_i)\right) \, \mathrm{meas}(\partial\omega_{s,i} \cap \partial\Omega) \tag{55b}$$

$$+ \, \sigma \, \epsilon(x_i) \, u_i^4 \, \mathrm{meas}\left(\omega_i \cap \Sigma\right) - \sum_{\alpha \in J_{\Sigma,i}} V_\alpha(\vec{u}\restriction_{I_\Sigma}) \tag{55c}$$

$$- \sum_{m \in \{s,g\}} f_m(x_i) \, \mathrm{meas}(\omega_{m,i}). \tag{55d}$$

5   Numerical Simulation

As discussed before, the modeling of conductive-radiative heat transfer is motivated by industrial applications such as crystal growth. We now present simulation results, where the solution θ to (18) has been computed and optimized numerically in the context of such applications for axisymmetric geometries. Here, the heat sources f are due to induction heating, generated by finitely many coil rings located outside the domain Ω. The heat sources are numerically computed according to the following model, where all materials in Ω_s are considered as potential conductors, whereas Ω_g is treated as a perfect insulator (see [2, Sec. 2.6] for details; due to the axisymmetry, cylindrical coordinates (r, z) are used):

$$f(r, z) = \frac{|j(r, z)|^2}{2 \, \sigma_c(r, z)}, \tag{56}$$

$$j = \begin{cases} -i\omega \, \sigma_c \, \phi + \frac{\sigma_c \, v_k}{2\pi r} & \text{in the } k\text{-th coil ring}, \\ -i\omega \, \sigma_c \, \phi & \text{in } \Omega_s, \end{cases} \tag{57}$$

where σ_c denotes the electrical conductivity, v_k is the voltage imposed in the kth coil ring, ω is the common angular frequency of the imposed voltages, and i is the imaginary unit. The potential ϕ is determined from the following system of elliptic partial differential equations:

$$-\nu \operatorname{div} \frac{\nabla(r\phi)}{r^2} \qquad\qquad\qquad = 0 \quad \text{in } \Omega_\mathrm{g}, \tag{58a}$$

$$-\nu \operatorname{div} \frac{\nabla(r\phi)}{r^2} \qquad + \frac{i\,\omega\sigma_\mathrm{c}\phi}{r} \qquad = \frac{\sigma_\mathrm{c}\,v_k}{2\pi r^2} \quad \text{in the } k\text{-th coil ring}, \tag{58b}$$

$$-\nu \operatorname{div} \frac{\nabla(r\phi)}{r^2} \qquad + \frac{i\,\omega\sigma_\mathrm{c}\phi}{r} \qquad = 0 \quad \text{in } \Omega_\mathrm{s}, \tag{58c}$$

where ν denotes the magnetic reluctivity. The system (58) is completed by the interface conditions

$$\left(\frac{\nu\!\restriction_{\overline{\Omega}_i}}{r^2}\, \nabla(r\phi)\!\restriction_{\overline{\Omega}_i} \right) \bullet \vec{n}_{\Omega_i} = \left(\frac{\nu\!\restriction_{\overline{\Omega}_j}}{r^2}\, \nabla(r\phi)\!\restriction_{\overline{\Omega}_j} \right) \bullet \vec{n}_{\Omega_i}, \tag{59}$$

where Ω_i and Ω_j can be either Ω_g or subsets of Ω_s, representing different solid materials, as the magnetic reluctivity ν can be discontinuous at interfaces between such different solid materials. Moreover, the assumption $\phi = 0$ is used both on the symmetry axis $r = 0$ and sufficiently far from the growth apparatus (imposed as Dirichlet boundary condition).

A finite volume discretization as described in Sec. 4 above was used to compute the solution θ to (18), where Newton's method was used to solve (55). The computation of the nonlocal radiation terms involves the calculation of visibility and view factors. The method used is based on [1] and is described in [27, Sec. 4]. The discrete scheme was implemented as part of the software *WIAS-HiTNIHS*[1] which is based on the program package *pdelib* [28]. In particular, *pdelib* uses the grid generator *Triangle* [29] to produce constrained Delaunay triangulations of the domains, and it uses the sparse matrix solver *PARDISO* [30, 31] to solve the linear system arising from the linearization of the finite volume scheme via Newton's method.

Figure 6 depicts a numerical solution for the temperature field θ inside a complex Czochralski crystal growth apparatus (for crystal growth from melt [32]). As described above, the model equations (18) and (56) − (59) have been used for the computation.

---

[1]**H**igh **T**emperature **N**umerical **I**nduction **H**eating **S**imulator; pronunciation: ∼hitnice.
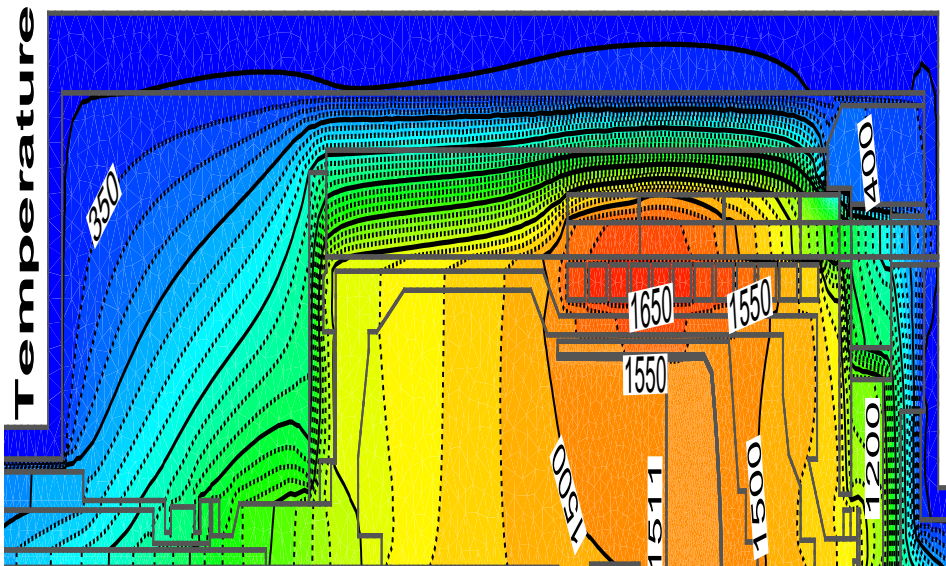
Figure 6: Numerical solution of (18) for the temperature field θ inside a Czochralski crystal growth arrangement computed by *WIAS-HiTNIHS*. The figure shows detail of an enlarged and rotated section, not according to scale – see [32] for the entire apparatus and the precise dimensions.

For the following numerical results of an optimal control problem, a simpler domain was used, schematically depicted in Fig. 7 (see [3, Figs. 1,3] for the precise dimensions). This domain represents an apparatus for silicon carbide single crystal growth via sublimation by physical vapor transport. As discussed in Sec. 3, during sublimation growth of silicon carbide, small horizontal temperature gradients in the gas domain Ω_g (more precisely in the part of Ω_g close to the surface of the growing crystal) are desirable to avoid defects of the growing crystal, while sufficiently large vertical temperature gradients are required to guarantee a material transport from the silicon source to the seed crystal [20, 21].
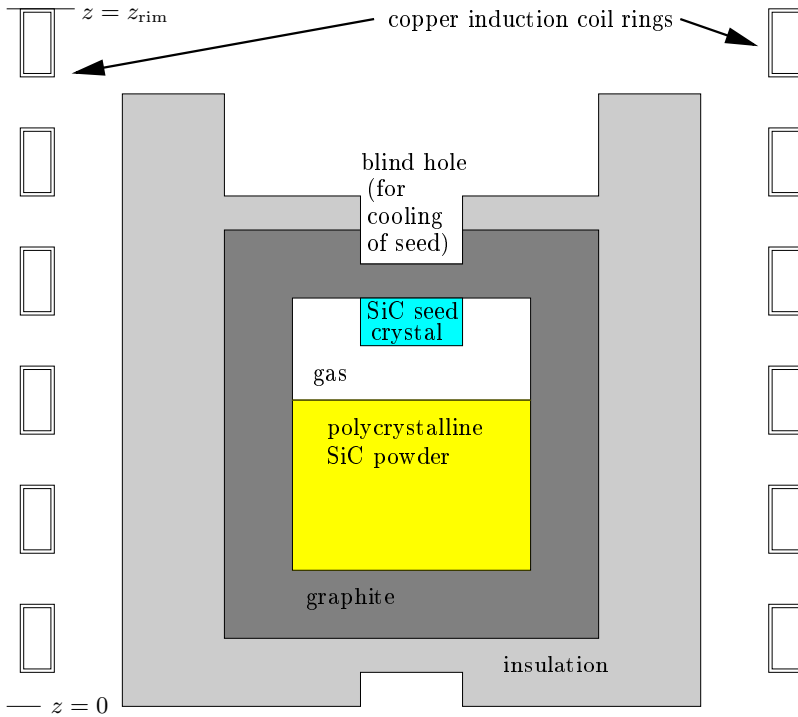
Figure 7: Schematic picture of apparatus for silicon carbide single crystal growth by physical vapor transport. For the precise dimensions of the domain used for the temperature field optimization, see [3, Figs. 1,3].

In the following, numerical optimization results from [3] are presented, where a problem similar to (28) was solved. However, for the numerical optimization of the temperature θ in [3], the heat sources were not controlled

directly as in (28), but they were computed according to (56) – (59), whereas the quantities heating power P, vertical upper rim z_{rim} of the induction coil (cf. Fig. 7), and the frequency $f = \omega/(2\pi)$ of the heating voltage were used as control parameters, which is more realistic from the point of view of the considered crystal growth application. The control parameters, thus, result in a temperature distribution $\theta(P, z_{\mathrm{rim}}, f)$ via (56) – (59) and (18) (see [3] for details).
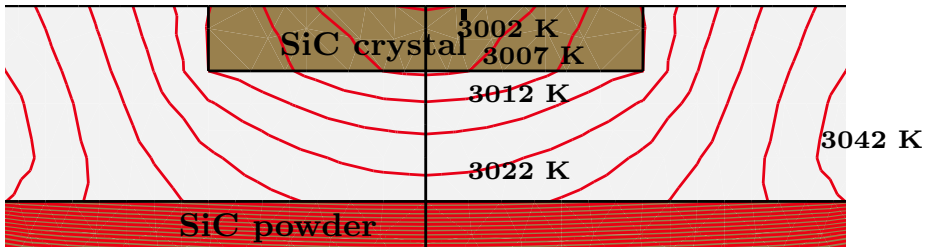
Figure 8: Stationary solution for the temperature field $\theta(P, z_{\mathrm{rim}}, f)$ in gas region A between SiC powder and crystal for the generic, unoptimized situation $P = 10$ kW, $z_{\mathrm{rim}} = 24$ cm, $f = 10$ kHz. Isotherms spaced at 5 K.

While Fig. 8 depicts the temperature field for a generic, unoptimized situation as a reference, the objective functional minimized in Fig. 9 is

$$\mathcal{F}_r(\theta) := \left(\int_{\Gamma} 2\pi\, r\, \partial_r\theta(r,z)^2 \,\mathrm{d}r \right)^{1/2}, \tag{60}$$

aiming at minimizing the radial temperature gradient on the lower surface Γ of the growing SiC crystal. The objective functional minimized in Fig. 10 is

$$\frac{1}{2}\mathcal{F}_r(\theta) - \frac{1}{2}\mathcal{F}_z(\theta), \quad \mathcal{F}_z(\theta) := \left(\int_A 2\pi\, r\, \partial_z\theta(r,z)^2 \,\mathrm{d}(r,z) \right)^{1/2}, \tag{61}$$

aiming at minimizing the radial temperature gradient on Γ, while simultaneously maximizing the vertical temperature gradient inside the region A between the SiC crystal and the SiC powder, to guarantee material transport from the powder to the crystal.

The optimization is subject to a number of state constraints on θ: (a) The maximal temperature in the apparatus must not surpass a prescribed bound $\theta_{\max}$; (b) the temperature at the crystal surface Γ needs to stay within a
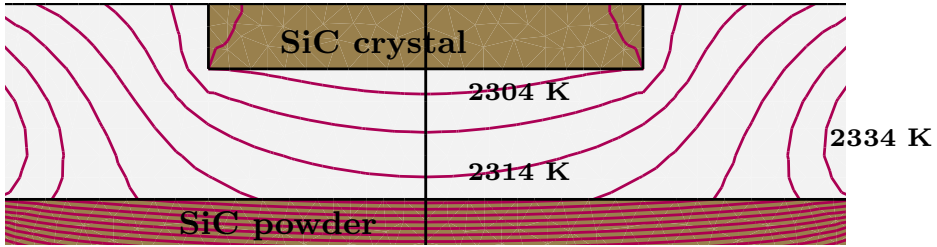
Figure 9: Temperature field $\theta(P, z_{\text{rim}}, f)$ in gas region A between SiC powder and crystal according to Nelder-Mead minimization of $\mathcal{F}_r(\theta)$, resulting in $P = 7.98$ kW, $z_{\text{rim}} = 22.7$ cm, $f = 165$ kHz. Isotherms spaced at 5 K.

prescribed range $[\theta_{\text{min},\Gamma}, \theta_{\text{max},\Gamma}]$; (c) the temperature gradient between source and seed must be negative, and must not surpass a prescribed value $\Delta_{\text{max}} < 0$:

$$\max_{\Omega}(\theta) \leq \theta_{\text{max}}, \tag{62a}$$

$$\theta_{\text{min},\Gamma} \leq \min_{\Gamma}(\theta) \leq \max_{\Gamma}(\theta) \leq \theta_{\text{max},\Gamma}, \tag{62b}$$

$$\max_{A}(\partial_z \theta) \leq \Delta_{\text{max}} < 0. \tag{62c}$$

A Nelder-Mead method was used for the numerical optimization as described in [3, Sec. 3].
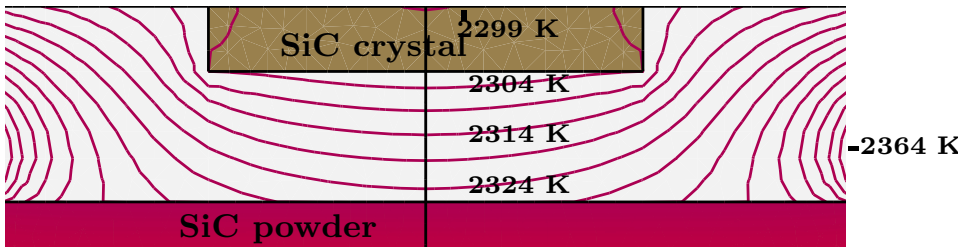

Figure 10: Temperature field $\theta(P, z_{\text{rim}}, f)$ in gas region A between SiC powder and crystal according to Nelder-Mead minimization of $\frac{1}{2}\mathcal{F}_r(\theta) - \frac{1}{2}\mathcal{F}_z(\theta)$, resulting in $P = 10.3$ kW, $z_{\text{rim}} = 12.9$ cm, $f = 84.9$ kHz. Isotherms spaced at 5 K.

The main difference between the generic solution of Fig. 8 and the op-

timized solutions shown in Figures 9,10 is the gained homogeneity of the temperature inside the SiC crystal in the optimized solutions (favorable with respect to low thermal stress and few crystal defects) as well as the isotherms below the crystal's surface becoming more parallel to that surface (as intended by the minimization of $\mathcal{F}_r(\theta)$). As expected, in Fig. 10, the maximization of $\mathcal{F}_z(\theta)$ leads to an increased number of isotherms between the crystal and the source powder. Summarizing the results, the radial and the vertical gradient can be effectively tuned simultaneously.

References

[1] F. Dupret, P. Nicodéme, Y. Ryckmans, P. Wouters, and M.J. Crochet. Global modelling of heat transfer in crystal growth furnaces. *Intern. J. Heat Mass Transfer*, 33(9):1849–1871, 1990.

[2] O. Klein, P. Philip, and J. Sprekels. Modeling and simulation of sublimation growth of SiC bulk single crystals. *Interfaces and Free Boundaries*, 6:295–314, 2004.

[3] C. Meyer and P. Philip. Optimizing the temperature profile during sublimation growth of SiC single crystals: Control of heating power, frequency, and coil position. *Crystal Growth & Design*, 5(3):1145–1156, 2005.

[4] C. Meyer, P. Philip, and F. Tröltzsch. Optimal control of a semilinear PDE with nonlocal radiation interface conditions. *SIAM J. Control Optim.*, 45:699–721, 2006.

[5] M. Metzger. Existence for a time-dependent heat equation with nonlocal radiation terms. *Math. Meth. Appl. Sci.*, 22:1101–1119, 1999.

[6] M. Laitinen and T. Tiihonen. Conductive-radiative heat transfer in grey materials. *Quart. Appl. Math.*, 59(4):737–768, 2001.

[7] J. Monnier and J.P. Vila. Convective and radiative thermal transfer with multiple reflections. Analysis and approximation by a finite element method. *Math. Models Methods Appl. Sci.*, 11(2):229–262, 2001.

[8] P.-É. Druet. *Analysis of a coupled system of partial differential equations modeling the interaction between melt flow, global heat transfer and*

applied magnetic fields in crystal growth. PhD thesis, Department of
Mathematics, Humboldt University of Berlin, Germany, 2008. Available
in pdf format at
`http://edoc.hu-berlin.de/dissertationen/druet-pierre-etienne-200`
`9-02-05/PDF/druet.pdf`.

 [9] P.-É. Druet. Weak solutions to a time-dependent heat equation with
nonlocal radiation boundary condition and arbitrary p-summable right-
hand side. *Applications of Mathematics*, 55(2):111–149, 2010.

[10] A.A. Amosov. Nonstationary nonlinear nonlocal problem of radiative-
conductive heat transfer in a system of opaque bodies with properties
depending on the radiation frequency. *Journal of Mathematical Sciences*,
165(3):1–41, 2010.

[11] A.A. Amosov. Stationary nonlinear nonlocal problem of radiative-
conductive heat transfer in a system of opaque bodies with properties
depending on the radiation frequency. *Journal of Mathematical Sciences*,
164(3):309–344, 2010.

[12] P.-É. Druet, O. Klein, J. Sprekels, F. Tröltzsch, and I. Yousept. Op-
timal control of 3D state-constrained induction heating problems with
nonlocal radiation effects. Preprint No. 1422, Weierstrass Institute for
Applied Analysis and Stochastics (WIAS), Berlin, 2009. Submitted to
SIAM J. Control Optim. Available in pdf format at
`http://www.wias-berlin.de/preprint/1422/wias_preprints_1422.pdf`.

[13] D. Schulz, M. Lechner, H.-J. Rost, D. Siche, and J. Wollweber. On
the early stages of sublimation growth of 4H-SiC using 8° off-oriented
substrates. *Mater. Sci. Forum*, 433–436:17–20, 2003. Proceedings of
4th European Conference on Silicon Carbide and Related Materials,
September 2–5, 2002, Linköping, Sweden.

[14] T. Tiihonen. A nonlocal problem arising from heat radiation on non-
convex surfaces. *Eur. J. App. Math.*, 8(4):403–416, 1997.

[15] T. Tiihonen. Stefan-boltzmann radiation on non-convex surfaces. *Math.
Meth. in Appl. Sci.*, 20(1):47–57, 1997.

[16] P.-É. Druet and P. Philip. Noncompactness of integral operators modeling diffuse-gray radiation in polyhedral and transient settings. Integr. Equ. Oper. Theory, in press. Published online July 14, 2010, DOI: 10.1007/s00020-010-1821-8.

[17] O. Klein and P. Philip. Transient conductive-radiative heat transfer: Discrete existence and uniqueness for a finite volume scheme. *Math. Mod. Meth. Appl. Sci.*, 15(2):227–258, 2005.

[18] P.-É. Druet. Weak solutions to a stationary heat equation with nonlocal radiation boundary condition and right-hand side in L^p ($p \geq 1$). *Math. Meth. Appl. Sci.*, 32(2):135–166, 2009.

[19] P.-É. Druet. Weak solutions to a stationary heat equation with nonlocal radiation boundary condition and right-hand side in L^p ($p \geq 1$). Preprint No. 1240, Weierstrass Institute for Applied Analysis and Stochastics (WIAS), Berlin, 2007, revised 2009. Available in pdf format at http://www.wias-berlin.de/preprint/1240/wias_preprints_1240.pdf.

[20] M. Selder, L. Kadinski, Yu. Makarov, F. Durst, P. Wellmann, T. Straubinger, D. Hoffmann, S. Karpov, and M. Ramm. Global numerical simulation of heat and mass transfer for SiC bulk crystal growth by PVT. *J. Crystal Growth*, 211:333–338, 2000.

[21] R. Ma, H. Zhang, V. Prasad, and M. Dudley. Growth kinetics and thermal stress in the sublimation growth of silicon carbide. *Crystal Growth & Design*, 2(3):213–220, 2002.

[22] C. Meyer. Second-order sufficient optimality conditions for a semilinear optimal control problem with nonlocal radiation interface conditions. *ESAIM: Optim. Calc. Var.*, 13:750–775, 2007.

[23] C. Meyer and I. Yousept. State-constrained optimal control of semilinear elliptic equations with nonlocal radiation interface conditions. *SIAM J. Control Optim.*, 48:734–755, 2009.

[24] P. Philip. *Transient Numerical Simulation of Sublimation Growth of SiC Bulk Single Crystals. Modeling, Finite Volume Method, Results.* PhD thesis, Department of Mathematics, Humboldt University of Berlin, Germany, 2003. Report No. 22, Weierstrass Institute for Applied Analysis

and Stochastics (WIAS), Berlin. Available in pdf format at
`http://www.wias-berlin.de/report/22/wias_reports_22.pdf`.

[25] O. Klein and P. Philip. Transient numerical investigation of induction heating during sublimation growth of silicon carbide single crystals. *J. Crystal Growth*, 247(1–2):219–235, 2003.

[26] J. Geiser, O. Klein, and P. Philip. Transient numerical study of temperature gradients during sublimation growth of SiC: Dependence on apparatus design. *J. Crystal Growth*, 297:20–32, 2006.

[27] O. Klein, P. Philip, J. Sprekels, and K. Wilmański. Radiation- and convection-driven transient heat transfer during sublimation growth of silicon carbide single crystals. *J. Crystal Growth*, 222(4):832–851, 2001.

[28] J. Fuhrmann, Th. Koprucki, and H. Langmach. pdelib: An open modular tool box for the numerical solution of partial differential equations. Design patterns. In W. Hackbusch and G. Wittum, editors. *Proceedings of the 14th GAMM Seminar on Concepts of Numerical Software, Kiel, January 23–25, 1998*, University of Kiel, Germany, 2001.

[29] J.R. Shewchuk. Triangle: Engineering a 2D Quality Mesh Generator and Delaunay Triangulator. In M.C. Lin and D. Manocha, editors. *Applied Computational Geometry: Towards Geometric Engineering*, Vol. 1148 of Lecture Notes in Computer Science, pp. 203-222, Springer-Verlag, Berlin, 1996.

[30] O. Schenk, K. Gärtner, and W. Fichtner. Scalable parallel sparse factorization with left-strategy on shared memory multiprocessor. *BIT*, 40(1):158–176, 2000.

[31] O. Schenk and K. Gärtner. Solving unsymmetric sparse systems of linear equations with PARDISO. *Journal of Future Generation Computer Systems*, 20(3):475–487, 2004.

[32] O. Klein, Ch. Lechner, P.-E. Druet, P. Philip, J. Sprekels, Ch. Frank-Rotsch, F.-M. Kießling, W. Miller, U. Rehse, and P. Rudolph. Numerical simulation of Czochralski crystal growth under the influence of a traveling magnetic field generated by an internal heater-magnet module (HMM). *J. Crystal Growth*, 310:1523–1532, 2008. Special Issue:

Proceedings of the 15th International Conference on Crystal Growth (ICCG-15) in conjunction with the International Conference on Vapor Growth and Epitaxy and the US Biennial Workshop on Organometallic Vapor Phase Epitaxy, Salt Lake City, USA, August 12-17, 2007.

[33] M. Pons, M. Anikin, K. Chourou, J.M. Dedulle, R. Madar, E. Blanquet, A. Pisch, C. Bernard, P. Grosse, C. Faure, G. Basset, and Y. Grange. State of the art in the modelling of SiC sublimation growth. *Mater. Sci. Eng. B*, 61-62:18–28, 1999.